Yang et al. Sustainable Environment Research (2022) 32:12
https://doi.org/10.1186/s42834-022-00119-w

Sustainable Environment Research

RESEARCH Open Access

Influence of aqueous chloride and bromide ions on bisphenol A degradation efficiency with zinc oxide nanoparticles

Yi-Chen Yang, Rama Shanker Sahu and Yang-hsin Shih*

Abstract

Zinc oxide (ZnO) nanoparticles (NPs) have been widely investigated for applications in photocatalytic degradation of organic pollutants in wastewater. Despite the advantages of robust ZnO material, its photocatalytic activity is greatly affected by environmental factors. Halogen ions are commonly found in wastewater, which directly affect the pollutant aggregation and sedimentation, therefore it is necessary to discuss their effect on the photocatalytic degradation. The current study assesses the halogen ions effect on the photocatalytic degradation of bisphenol A (BPA) using different dosage of sodium chloride (NaCl) and sodium bromide (NaBr). The microstructural characterization of ZnO NPs was conducted by transmission electron microscopy and hydrodynamic size was analyzed through dynamic light scattering. The effective BPA degradation with ZnO NPs was observed and pseudo-first-order kinetics was calculated. The increase of ZnO NPs dosage from 10 to 100 mg L^{-1} enhanced the degradation rate constant of BPA up to 0.089 min^{-1} (14.8 folds). In order to evaluate the role halogen ions to degrade BPA, NaBr and NaCl were used. The degradation rate was reduced to 0.0034 min^{-1} after the addition of NaBr due to the increase in hydrodynamic particle size, thereby restricting the light adsorption capacity. Noteworthy, upon addition of NaCl up to 500 mM concentration, only a slight decrease on BPA degradation rate was observed. Therefore, this study unveils the role of chloride ions as an effective medium for BPA degradation by ZnO NPs, without aggregation, and provides a novel platform for the treatment of organic pollutants in saline water.

Keywords: BPA, Zinc oxide, Photocatalytic degradation, Inorganic ion, Hydrodynamic particle size

1 Introduction

World-wide contamination of phenolic compounds in aquatic environmental has attracted increasing attentions in the research society. Bisphenol A (BPA) used as basic monomer in the synthesis of brominated flame retardants, epoxy resins and polycarbonates due to which it became the highest produced chemical worldwide [1]. However, their characteristics, environmental distribution and adverse effect on human health remain less-known compared to conventional pollutants with the worldwide demand dramatically increasing [2]. BPA is one of the endocrine disruptors due to its genotoxic and estrogenic activity, which damage the reproduction and brain development [3]. Owning to the discharge of wastewater and improper accumulation of solid waste, BPA has been ubiquitous in the environment [4]. In some rivers, BPA concentration could even reach up to 8 μg L^{-1} [5], and the report from Barboza et al. [6] also revealed the present of BPA and its analogs in muscle and liver of fish. In China, up to 144 ng mL^{-1} of bisphenol analogues was detected in serum samples from pregnant women [7]. Since even low concentration of BPA causes hazardous health, the development of treatment techniques with high efficiency is required.

Treatment of contaminated wastewater has received increasing attention. Several techniques such as chemical oxidation [8], sono-photo-Fenton oxidation [9], UV-

* Correspondence: yhs@ntu.edu.tw
Department of Agricultural Chemistry, National Taiwan University, Taipei 106, Taiwan

assisted chemical oxidation [10], electrochemical degradation [11], zerovalent metal-based reduction [12], biodegradation [13], and adsorption methods [14] were studied. Chemical oxidation method has been widely used for wastewater treatment including Fenton process [15] and ozone treatment [16] process, which could effectively oxidize the organic contaminants in the wastewater. Nanoscale zero valent iron (NZVI) has appropriate redox potential to reduce organic contaminant [17, 18, 19] under anaerobic conditions but cannot totally mineralize the contaminant due to its losing reducing activity and quick oxidation when exposed in the air. Previous studies reported that BPA is biodegradable by bacterial strains [20], while it takes at least several days to remove BPA and produces byproducts. Activated carbon is commonly used for adsorption of compounds in air or aquatic system and the adsorption capacity depends on the carbon used and the characteristic of wastewater [21, 22]. Physical adsorption is cost effective treatment procedure [23] but the contaminated adsorbent requires further treatment and proper disposal. Various studies suggest that chemical reduction, advanced oxidation and electrochemical processes are desired and effective treatment procedure for BPA, which could be activated by using expensive and noble metal catalysts [24]. Park et al. have demonstrated improved photocatalytic degradation of BPA in the presence of silver nanoparticles (NPs) immobilized with polyvinyl alcohol and activated by low hydrogen peroxide (H_2O_2) concentration [25]. The quick dissolution of silver NPs was also reported due to the presence highly reactive H_2O_2 in the solution. NZVI has been exploited in last 4 decades for wastewater treatment but agglomeration due to intrinsic magnetic properties and quick aerial oxidation of NZVI remain the major challenges [26].

The natural phenomenon involves the direct photocatalytic degradation of organic chemicals in the environment. The photocatalysis is the most convenient method for the treatment of wastewater due to its facile procedure, inexpensive operational cost, high degradation efficacy facilitated by reactive oxygen species generated during the reaction. In this regard, zinc oxide (ZnO) NPs, an environmentally benign material has been used for photocatalytic degradation of organic pollutants from wastewater. ZnO NPs have attained the huge acceptance for environmental applications because of their remarkable optical properties, electron affinity, high redox potential, environmentally benign, and relatively low cost [27, 28]. The commercial or chemically modified ZnO NPs have demonstrated substantial differences in their morphology, shape and size, and photoelectric properties which show important role in the optical properties and photoactivity of ZnO NPs. However, previous studies showed that the effect of environmental factors such as pH, inorganic ions [29, 30, 31] and organic compounds are important and needed to be considered in the ZnO NPs photocatalytic degradation process. Wang et al. have uncovered the influence of different inorganic ions (PO_4^-, SO_4^{-2}, CO_3^-) on the degradation of BPA in the presence of ZnO NPs, in which PO_4^- ions restricted the BPA degradation to 10% [32]. It was observed that the adsorption of the dyes onto the surface of ZnO NPs is strongly influenced by the pH of the solution due to the surface charge of both ZnO NPs and contaminants [33]. The effect of inorganic ions on ZnO photocatalytic degradation has been widely reported, yet whether the addition of inorganic ions can increase or decrease degradation efficiency is still unsure in different conditions. Lee et al. [34] demonstrated the role of various inorganic species such as BrO_3^-, $S_2O_8^{2-}$ and SO_3^- could be advantageous to enhance the photocatalytic degradation of organic contaminants in the presence of ZnO NPs. However, some inorganic ions such as Cl^-, NO_3^- and CO_3^{2-} tend to retard the photocatalytic degradation of ZnO NPs. The anions have been known to be OH radical and photo-hole scavengers, strong reactive species for BPA degradation. In addition, the cations including Na^+, K^+, and Ca^+ slightly inhibit the BPA degradation by reducing the electrical double layer to enhance the ZnO NPs aggregation [35]. Therefore, it is noteworthy to evaluate the performance of ZnO-based photocatalysts in the presence of inorganic ions in the wastewater during the photocatalytic treatment process.

The current study demonstrates the effect of inorganic ions on the photocatalytic degradation of BPA using ZnO NPs under UV light irradiation. The effect of ZnO NPs dosages on photocatalytic degradation of BPA was investigated to optimize the optimum catalyst dose. The experiments under the influence of different inorganic ion concentrations (NaCl and NaBr) were performed and the change in hydrodynamic particle sizes were also monitored. The relationship among inorganic ion concentration, ZnO particle size and reaction kinetics is discussed.

2 Materials and methods

2.1 Materials

The commercial ZnO NPs powder (Uniregion Biotech) with particle size of 20 nm was used in the experiments. Bisphenol A (CAS No. 80–05-7), sodium chloride and sodium bromide in this research were obtained from Acros Organics. All solutions were prepared with ultrapure water and used without further purification.

2.2 Characterization of ZnO NPs analysis

The crystal patterns of the ZnO NPs were measured by Bruker D8 Advanced X-ray diffractometer (XRD) with

Cu-Kα radiation (Ni filtered, λ = 1.5405 Å, at voltage 40 kV and current 40 mA). The morphology of ZnO NPs was analyzed by transmission electron microscopy (TEM). NPs suspension was prepared using desired ZnO NPs concentrations and ultrasonicated for 10 min at room temperature. DELTA ultrasonic cleaning machine, DC150H/150 W was used for homogenous suspension. The hydrodynamic particle size of ZnO NPs and their distributions were measured by a dynamic light scattering (DLS) instrument (Zetasizer nano ZS, Malvern nano series V6.0). UV–Vis spectra was used to record the light absorption property of ZnO NPs under the wavelength between 200 to 800 nm. The sedimentation of those large agglomerates of ZnO NPs was also monitored with UV–Vis spectra at 365 nm in 90 min. High performance liquid chromatography (HPLC, Agilent 1200 series) equipped with C-18 column, auto-injector, and variable wavelength detector was used to analyze the concentration of BPA in the experiments.

2.3 Photocatalytic degradation experiments

The typical photocatalytic experiments were conducted in the laboratory. A photochemical reactor was equipped with 4 × 8-W UV lamps at the irradiation wavelength of 365 nm. Experimental solutions in 30 mL tubes were placed in a rotor inside the photochemical reactor to irradiate them equally. In degradation experiments, 25 mL solution that contained different ZnO NPs photocatalyst dosages (10–100 mg L^{-1}) and 5 ppm BPA was prepared to conduct the experiments. After 30-min dark adsorption experiment, the solutions were illuminated under the light at the irradiation wavelength of 365 nm. All the experiments were performed in 100 mg L^{-1} ZnO NPs dose, 5 ppm BPA conc., and neutral pH at room temperature until unless mentioned. During the experiment, the aliquot of 2 mL was collected, filtered through 0.22-μm filter and the concentration of BPA was analyzed by HPLC through auto-injector at selected intervals. In addition, Coumarin has been employed to detect ·OH radicals during the photocatalytic degradation of BPA. The fluorescence probe compound (coumarin) was used which upon reaction with ·OH radicals generated byproduct (7-hydroxycoumarin), measured by photoluminescence, as described in the literature [36]. In brief, 0.1 mM coumarin solution was taken as blank and desired amount of ZnO NPs was dispersed in the dark under continuous stirring. The aqueous solution was then exposed to UV light and aliquots were withdrawn at specific time intervals and filtered immediately. The obtained solution was then analyzed by fluorescence spectrophotometer (Hitachi, F-7000 FL spectrophotometer).

2.4 Chloride and bromide ions effect

NaCl and NaBr were used as inorganic ions under specific dosage of ZnO NPs to evaluate BPA degradation in the following experiments. Different chloride or bromide ion concentrations (0 to 500 mM) were used for BPA degradation process. Before performing the experiments, the inorganic ions and ZnO NPs were added to the solution containing 5 ppm BPA, stirred for 1 min and kept in the dark for 30 min to attain adsorption and desorption equilibrium before the photocatalytic degradation. The reaction solution was later exposed to UV light to observe the photocatalytic efficiency of ZnO NPs. The aliquot of 2 mL was collected, filtered through 0.22-μm filter and analyzed by HPLC through auto-injector at desired intervals. DLS and pH analysis were also carried out after every batch of experiment.

3 Results and discussion

3.1 Morphological characterization of ZnO NPs

The crystal patterns of ZnO NPs were analyzed by XRD as displayed in Fig. 1a. Various crystal patterns of ZnO NPs with high relative intensity have been observed at 31.8° (100), 34.6° (002), 36.3° (101), 48.2 (102), 56.6° (110), 62.6° (103), and 68.7° (112), consistent with JCPDS No. 36–1451 [32]. The TEM image of ZnO NPs in Fig. 1b demonstrates the clear particle distribution and also the formation of small clusters. However, due to the high surface potentials of ZnO NPs, they aggregate when store for long time and need further dispersion before every experiment. ZnO NPs aggregate to form big agglomerates and the particle sizes can approach microscale, when suspended in DI water. ZnO NPs aggregation was further analyzed by DLS (Fig. 1c), depicts the average particle size of ZnO NPs in water is about 250 nm after sonication. Many studies applied ultrasonication to suspend NPs in aqueous solution before experiments [37]. Therefore, ZnO NPs suspensions used in experiments was allowed for 30 min ultrasonication in advance to properly disperse NPs. The full-scale UV-Vsible spectra of ZnO NPs were obtained as depicted in Fig. 1d to confirm the light absorption range (365 nm), which is corresponding to a broad band gap (3.39 eV) in Choi et al.'s report [38].

3.2 Photocatalytic degradation of BPA

The photocatalytic degradation of 5 ppm BPA was performed by varying the dosage of ZnO NPs from 10 to 100 mg L^{-1} under 365 nm UV light (Fig. 2a). The degradation rate constants (k) were determined by a pseudo-first-order rate kinetics [39, 40]:

$$C = C_0 e^{-kt}$$

where C is the concentration of BPA after time t, C_0 is the initial concentration of BPA, t is the reaction time, and k is the pseudo-first-order rate kinetics.

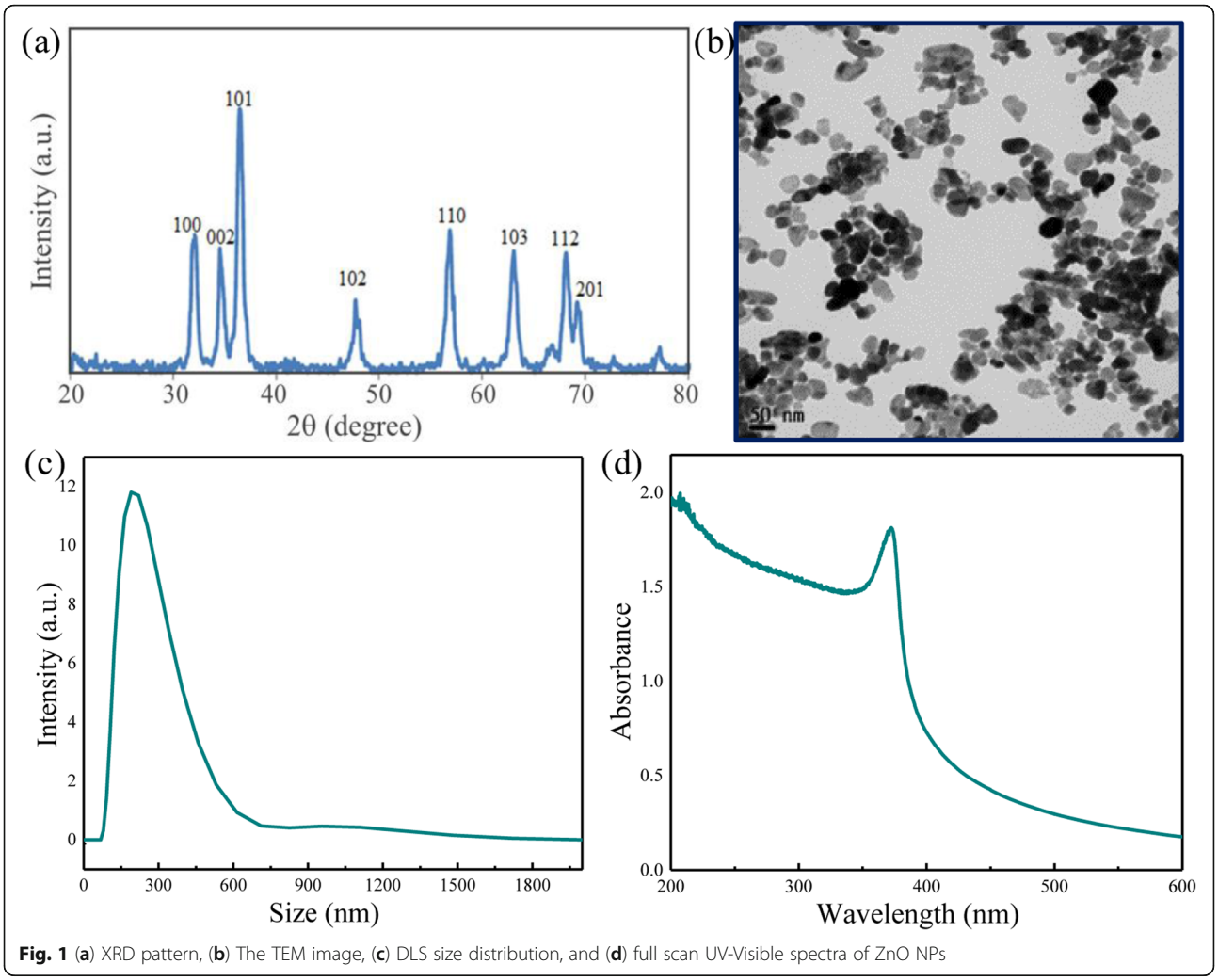

Fig. 1 (**a**) XRD pattern, (**b**) The TEM image, (**c**) DLS size distribution, and (**d**) full scan UV-Visible spectra of ZnO NPs

The photocatalytic degradation rate can be properly described by pseudo-first-order kinetics under different ZnO NPs dosages. Enhanced rate of BPA was observed when ZnO NPs dose increased from 10 to 100 mg L^{-1} (0.006 to 0.089 min^{-1}). Previous studies also indicated that photocatalytic degradation rates of NPs on organic contaminants can be described by pseudo-first-order kinetics [41, 42]. The enhancement of the degradation rate of BPA was observed with the increase of ZnO NPs dosage from 10 mg to 100 mg L^{-1}, owning to the increase in the concentration of catalyst and adsorption sites on ZnO NPs surface. The result of full scan also showed that the fraction of UV light absorbed by the catalyst increased as the concentration of ZnO NPs increased in a suspension (Fig. 2b). Therefore, 100 mg L^{-1} ZnO NPs catalyst dose was used during entire photocatalytic experiments. Previous studies indicate that OH radicals and positive holes play the major role in ZnO photocatalytic degradation process [43, 44]. Owing to the increased yield of OH radicals as the dosage of ZnO NPs increased, the proportion of reactive oxygen species that attack BPA and its intermediates increases. There was no significant adsorption was observed when the dosage of ZnO NPs was 20, 50 and 100 mg L^{-1}, while the removal of 7% BPA by 100 mg L^{-1} ZnO NPs was observed in the first 30 min under dark condition. Considering of economic efficiency, the following experiments were performed with the dosage of 100 mg L^{-1} ZnO NPs. The linear relationship between ZnO NPs concentration (10–100 mg L^{-1}) and k_{obs} (pseudo-first-order rate constant) can be observed. Figure 2c shows the rate of BPA enhances as catalyst dose increased from 10 mg L^{-1} (0.006 min^{-1}) to 100 mg L^{-1} (0.089 min^{-1}), suggesting the degradation of BPA is catalyst dose dependent. The reusability and stability of ZnO NPs have been analyzed by performing 3-consecutive BPA degradation cycles (Fig. 2d). 100 mg L^{-1} of ZnO NPs dispersed in the BPA (5 ppm) solutions under similar reaction conditions for reusability test. The sample aliquots were collected at selected time intervals during entire experiment. The

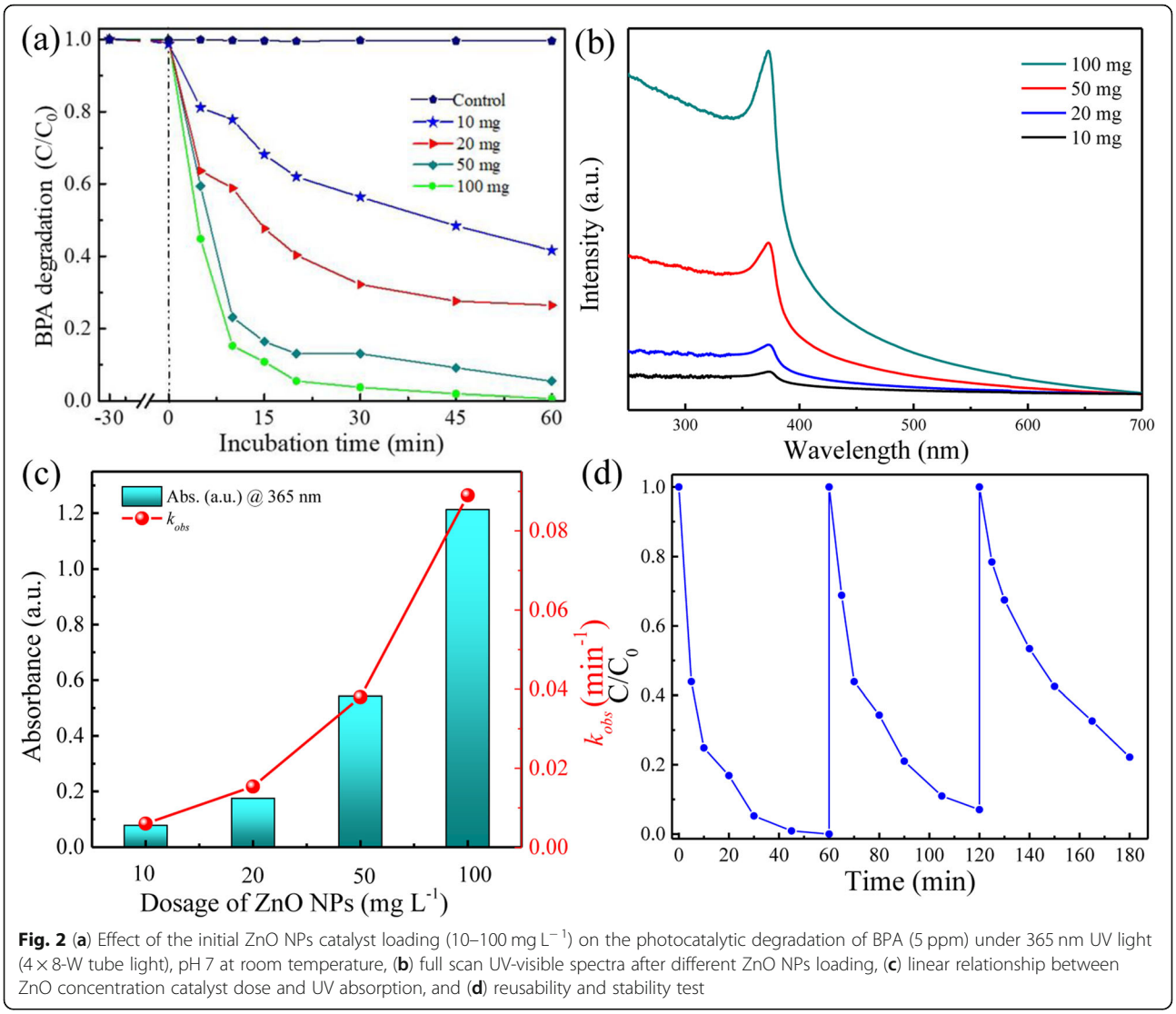

Fig. 2 (**a**) Effect of the initial ZnO NPs catalyst loading (10–100 mg L^{-1}) on the photocatalytic degradation of BPA (5 ppm) under 365 nm UV light (4 × 8-W tube light), pH 7 at room temperature, (**b**) full scan UV-visible spectra after different ZnO NPs loading, (**c**) linear relationship between ZnO concentration catalyst dose and UV absorption, and (**d**) reusability and stability test

initial BPA concentration was maintained to 5 ppm after each photocatalytic cycle. Slight decrease in the photocatalytic rate was observed after 3 repeated cycles, suggest that ZnO NPs can be utilized for BPA degradation repeatedly more than one cycle.

The ·OH radicals generated during BPA degradation were measured by PL probe method using coumarin. 100 mg ZnO NPs were dispersed in 0.1 mM coumarin solution and stirred under dark for 30 min before UV light illumination. The photogenerated 7-hydroxycoumarin compound were then collected and analyzed measuring PL signals. The excitation wavelength was set at 332 nm and scan range was selected between 380 to 600 nm with the scanning speed of 240 nm min^{-1}. Figure 3a shows the different PL curves of the solution obtained at different time period. The PL signal intensity increases as time increases, suggesting the formation of ·OH radicals in the solution. The change in fluorescence intensity (%ΔF) respective to time was analyzed and shown in Fig. 3b. the linear curve of fluorescence intensity change suggesting that ZnO NPs exposure under UV light generates ·OH radicals, which are responsible for BPA degradation. Our previous study demonstrates the enhanced photocatalytic BPA mineralization by metal-free graphitic carbon nitride was achieved due to the formation of ·OH radical, and byproducts were identified by high-resolution electrospray ionization mass spectrometry analysis [45].

3.3 The effect of chloride ions on photocatalytic degradation of BPA

The effect of different NaCl concentrations on the photocatalytic degradation process of BPA in the presence of ZnO NPs was evaluated. Figure 4a shows the increase of NaCl concentration resulting in slower BPA removal; the degradation rate constant was decreased around 50% by 500 mM NaCl. The BPA rate constants

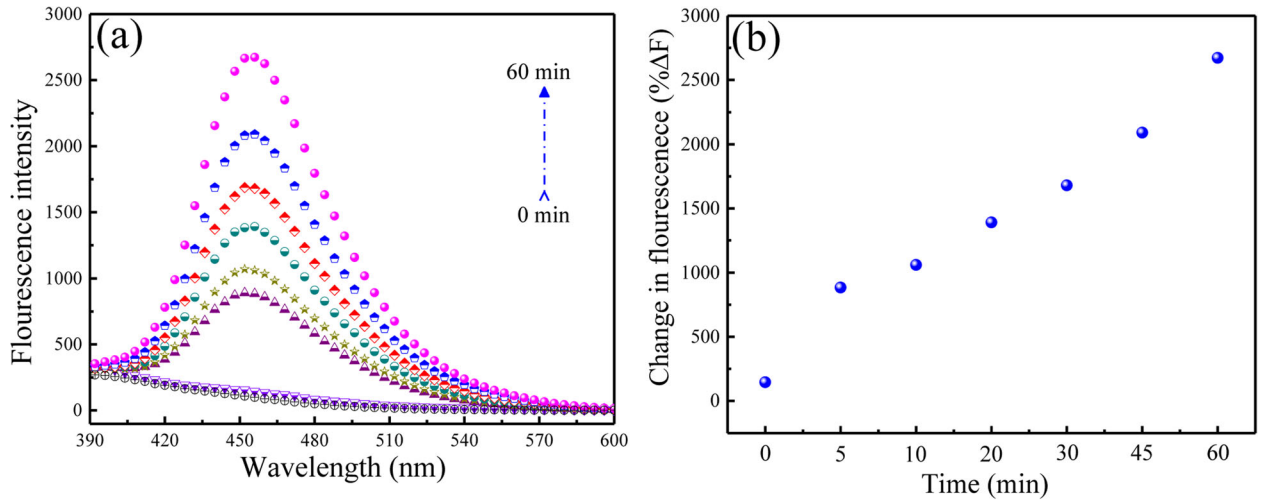

Fig. 3 (**a**) PL spectra of ZnO NPs at different time intervals, and (**b**) change in fluorescence intensity with time

were calculated 0.089, 0.038, 0.035 and 0.032 min^{-1} for 0, 10, 100 and 500 mM NaCl, respectively (Fig. 4b and Table 1). The previous studies reported that in the presence of inorganic ions, the compression of the electrostatic double layer of NPs occurs, causing particle aggregation, decrease of surface area and therefore the decline of the photocatalytic degradation activity [46, 47]. The effect of NaCl on ZnO NPs was investigated and observed the absorbance change over time. The average hydrodynamic particle size of ZnO NPs after degradation experiments were determined by UV-Visible spectra and DLS. Furthermore, ZnO NPs sedimentation was also observed in the presence of various NaCl concentrations. The absorbance decreased up to 32% when NaCl concentration increased to 500 mM NaCl concentration after 90 min sedimentation time (Fig. 5a). On the other hand, the average hydrodynamic particle sizes were 1240, 1421, 1330 and 1265 nm for 0, 10, 100, and 500 mM addition of NaCl, respectively (Fig. 5b and Table 1). The decreasing trend of the absorbance of ZnO NPs indicated the settlement of ZnO NPs with the increasing of NaCl concentration. However, there was no significant enhancement in the aggregation behavior showed in DLS result when the addition of NaCl concentration increased up to 500 mM, which was consistent with the result of absorbance change and the slightly suppression on degradation rate constants. The dual effect of NaCl on photocatalytic degradation was also observed by Liu et al. [48]. Chloride ions could enhance or suppress the degradation of Acid Orange 7 in different

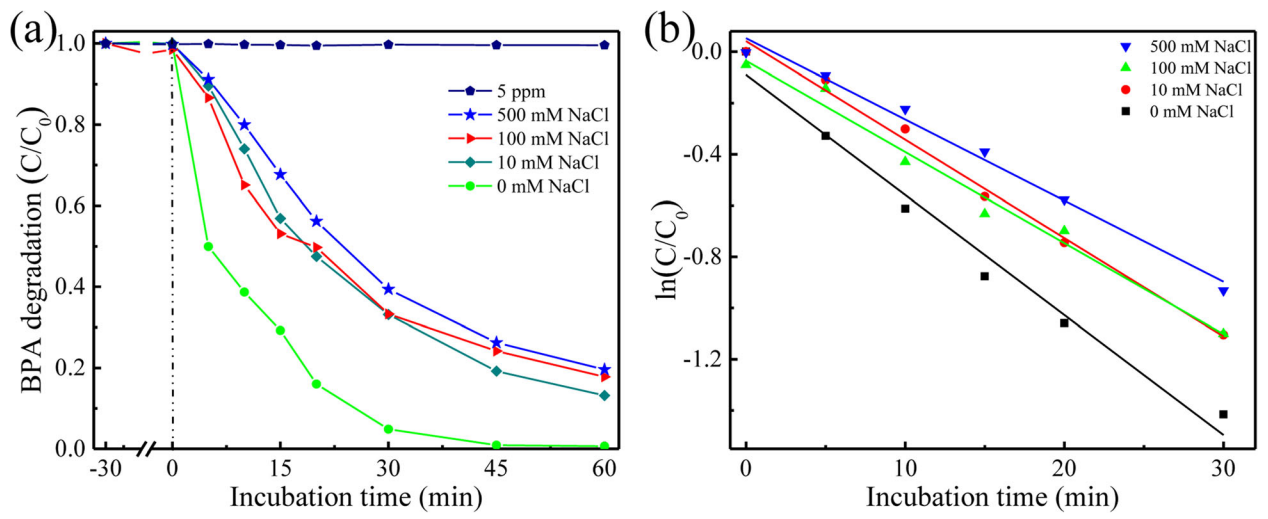

Fig. 4 (**a**) Effect of the NaCl concentration on the photocatalytic degradation of BPA with ZnO NPs under 365 nm UV light, (**b**) the plot of ln (C/Co) vs irradiation time for the photocatalytic degradation of BPA with ZnO NPs under different NaCl concentrations

Table 1 Effect of NaCl and NaBr on the observed rate constant (min^{-1}), final average particle size (nm) measured by DLS, and the final pH

	Salt dosage (mM)	Kinetic constant (min^{-1})	Final particle size (nm)	Final pH
NaCl	0	0.089	1240	6.70
	10	0.046	1421	6.95
	100	0.038	1330	7.2
	500	0.032	1265	7.45
NaBr	0	0.089	1240	6.70
	10	0.0076	1935	6.75
	100	0.0053	2399	6.98
	500	0.0038	2115	6.85

*Initial reaction pH 6.7

systems [49]. The higher NaCl concentration (> 50 mM) is beneficial to increase the amount of reactive chlorine species, while the dye photocatalytic degradation rate decreased with low NaCl concentration (< 10 mM), signifying that the concentration impacts the effect of NaCl on the photocatalytic degradation [50].

3.4 The effect of sodium bromide on photocatalytic degradation of BPA

Experiments of different NaBr concentration on the photocatalytic degradation performances of ZnO on BPA was carried out and shown in Fig. 6a. Upon addition of NaBr from 10 to 500 mM concentration, the degradation of BPA was found to be suppressing, suggesting a reaction constraining effect. This inhibition could be due to the competition between BPA molecules and bromide ions on the active sites of the catalysts. The photogenerated rate constants were 0.089, 0.0076, 0.0053 and 0.0038 min^{-1} for 0, 10, 100 and 500 mM NaBr addition, respectively (Fig. 6b and Table 1). The suppression effect of NaBr on BPA degradation was noticeably seen, which was in the following sequence 10 > 100 > 500 mM. In order to observe the hydrodynamic changes of the ZnO NPS, which may affect the surface area and active sites, the DLS study was conducted. The results clearly showed the increase of the average hydrodynamic size of ZnO NPs after the addition of NaBr. The sedimentation curve of solution indicates the aggregation of ZnO NPs, which could be the reason for the suppression of BPA degradation reaction (Fig. 7a). Further, the average hydrodynamic size of ZnO NPs was found to be 1240 nm for 0 mM NaBr, 1935 nm for 10 mM NaBr, 2399 nm for 100 mM NaBr and 2115 nm for 500 mM NaBr (Fig. 7b and Table 1). These results show that the BPA photocatalytic degradation depends on the ion concentration. The presence of NaCl and NaBr also causes the salting-out effect, resulting in the insolubility of BPA, hence decrease the photocatalytic degradation [51]. Garcia-Espinoza et al. [52] demonstrated the striking effect of halide ions for dye degradation due to

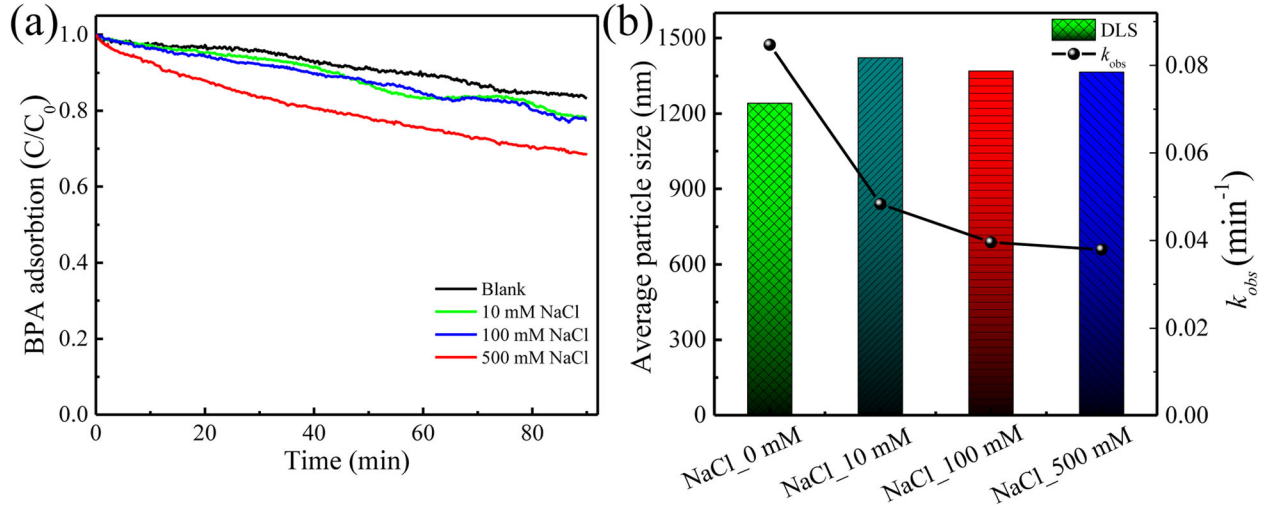

Fig. 5 (**a**) Sedimentation curve of ZnO NPs after loading different NaCl concentration, (**b**) effect of NaCl on average particle size distribution of ZnO NPs and the photocatalytic degradation rate constants

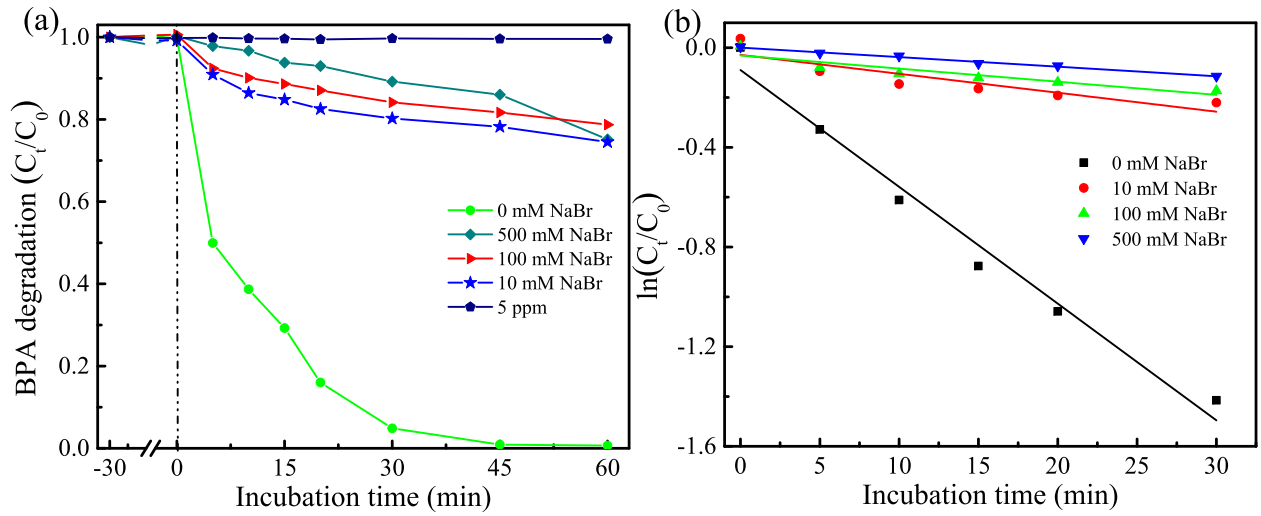

Fig. 6 (**a**) Effect of the NaBr concentration on the photocatalytic degradation of BPA under 365 nm UV light, (**b**) the plot of ln (C/Co) vs irradiation time for the photocatalytic degradation of BPA with ZnO NPs under different NaBr concentrations

halide radical formation. This study of the inorganic ion effect (usually negative) over BPA photocatalytic degradation is found to be supporting the degradation process (in the presence of NaCl), by ZnO NPs, hence providing a novel platform for better understanding of the inorganic ion-based wastewater treatment.

4 Conclusions

The photocatalytic degradation kinetic rate constant of BPA increased with the increase of ZnO NPs dosages from 10 to 100 mg L^{-1}, with insignificant adsorption during 30 min dark experiment. An obvious aggregation was observed after aqueous dispersion of ZnO NPs, leading to formation of large particles, contrary to the commercial 20 nm particle size. The effect of halide ions during photocatalytic degradation of BPA was investigated using NaCl and NaBr salt solutions. NaBr salt solution restricts the BPA degradation due to aggregation and limited light adsorption capacity. The average hydrodynamic particle size of ZnO NPs increased around 139%, leading to reduced rate of BPA up to 90% compared to the one without NaBr. However, NaCl could slightly suppress the degradation rate of BPA around 50% by 500 mM NaCl. The sedimentation curve reveals no significant change on the particle size and light absorbance efficiency, suggesting the relation between the rate constant and the average hydrodynamic particle size. Suppressed rate of BPA could be

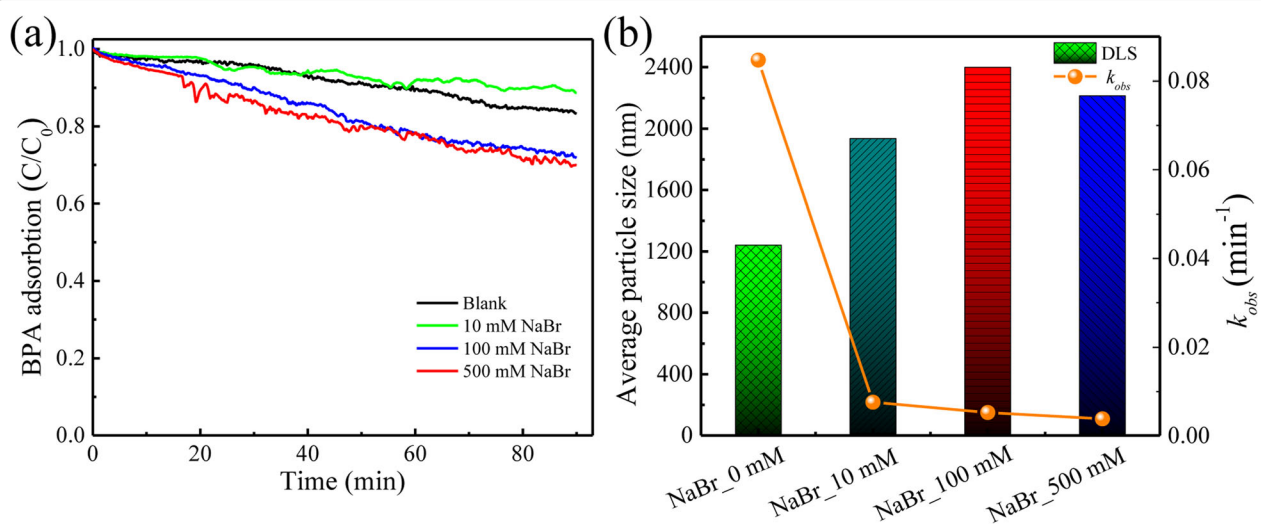

Fig. 7 (**a**) Sedimentation curve of ZnO NPs after loading different NaBr concentration, (**b**) effect of NaBr loading on average particle size distribution of ZnO NPs and the photocatalytic degradation rate constants

anticipated due to competition between NaCl salt and BPA molecules. This study reveals the impact of NaCl and NaBr salt solution on BPA removal and provides an essential information to facilitate the remediation of inorganic ion-included wastewater in the future.

Acknowledgments
The authors gratefully acknowledge the financial support of the Ministry of Science and Technology, Taiwan, Ms. Chia-ying Chien in Instrumentation Center (National Taiwan University) for the assistance in TEM experiment. We appreciate the help from Mr. Bo-Yen Chen for his experimental work during dose and pH optimization. We thank the anonymous referees for reviewing this manuscript.

Authors' contributions
Yi-Chen Yang and Rama Shanker Sahu provide equal contribution for this paper. Yi-Chen Yang: Conducted experiment, analyzed data, and wrote the manuscript draft. Rama Shanker Sahu: designed some experiments, analyzed data and wrote the manuscript, and Yang-Hsin Shih: Conceptualize, design, and corrected the manuscript. All authors read and approved the final manuscript.

Funding
Yi-Chen Yang thanks her college student research funding from Ministry of Science and Technology, Taiwan.

Availability of data and materials
All data generated or analyzed during this study are included in the manuscript.

Declarations

Competing interests
The authors declare they have no competing interests.

Received: 12 April 2021 Accepted: 29 December 2021
Published online: 28 January 2022

References
1. Liu G, Hyotylainen T, Falandysz J. Toxicology and environmental characteristics of emerging pollutants. Ecotox Environ Safe. 2019;181:264.
2. Yang SQ, Cui YH, Liu YY, Liu ZQ, Li XY. Electrochemical generation of persulfate and its performance on 4-bromophenol treatment. Sep Purif Technol. 2018;207:461–9.
3. Chouhan S, Yadav SK, Prakash J, Swati, Singh SP. Effect of Bisphenol A on human health and its degradation by microorganisms: a review. Ann Microbiol. 2014;64:13–21.
4. Lee CC, Hsieh CY, Chen CS, Tien CJ. Emergent contaminants in sediments and fishes from the Tamsui River (Taiwan): their spatial-temporal distribution and risk to aquatic ecosystems and human health. Environ Pollut. 2020;258:113733.
5. Huang YQ, Wong CKC, Zheng JS, Bouwman H, Barra R, Wahlstrom B, et al. Bisphenol A (BPA) in China: a review of sources, environmental levels, and potential human health impacts. Environ Int. 2012;42:91–9.
6. Barboza LGA, Cunha SC, Monteiro C, Fernandes JO, Guilhermino L. Bisphenol A and its analogs in muscle and liver of fish from the North East Atlantic Ocean in relation to microplastic contamination. Exposure and risk to human consumers. J Hazard Mater. 2020;393:122419.
7. Li AJ, Zhuang TF, Shi W, Liang Y, Liao CY, Song MY, et al. Serum concentration of bisphenol analogues in pregnant women in China. Sci Total Environ. 2020;707:136100.
8. Angeles LF, Mullen RA, Huang IJ, Wilson C, Khuniar W, Sirotkin HI, et al. Assessing pharmaceutical removal and reduction in toxicity provided by advanced wastewater treatment systems. Environ Sci-Wat Res. 2020;6:62–77.
9. Dukkanci M. Sono-photo-Fenton oxidation of bisphenol-A over a $LaFeO_3$ perovskite catalyst. Ultrason Sonochem. 2018;40:110–6.
10. Kaur B, Dulova N. UV-assisted chemical oxidation of antihypertensive losartan in water. J Environ Manage. 2020;261:110170.
11. Gui L, Jin HY, Zheng Y, Peng RC, Luo YB, Yu P. Electrochemical degradation of bisphenol A using different modified anodes based on titanium in aqueous solution. Int J Electrochem Sc. 2018;13:7141–56.
12. Bao T, Damtie MM, Hosseinzadeh A, Wei W, Jin J, Vo HNP, et al. Bentonite-supported nano zero-valent iron composite as a green catalyst for bisphenol A degradation: preparation, performance, and mechanism of action. J Environ Manage. 2020;260:110105.
13. Garcia-Becerra FY, Ortiz I. Biodegradation of emerging organic micropollutants in nonconventional biological wastewater treatment: a critical review. Environ Eng Sci. 2018;35:1012–36.
14. Lee JH, Kwak SY. Rapid adsorption of bisphenol A from wastewater by beta-cyclodextrin-functionalized mesoporous magnetic clusters. Appl Surf Sci. 2019;467:178–84.
15. Chmayssem A, Taha S, Hauchard D. Scaled-up electrochemical reactor with a fixed bed three-dimensional cathode for electro-Fenton process: application to the treatment of bisphenol A. Electrochim Acta. 2017;225:435–42.
16. Akbari S, Ghanbari F, Moradi M. Bisphenol A degradation in aqueous solutions by electrogenerated ferrous ion activated ozone, hydrogen peroxide and persulfate: applying low current density for oxidation mechanism. Chem Eng J. 2016;294:298–307.
17. Shih YH, Chen M. Effects of cation on dechlorination of pentachlorophenol by nanoscale Pd/Fe bimetallic particles. Sustainable Environment Research, 2010, 20: 333-339.
18. Shih YH, Tso CP, Tung LY, Rapid Degradation of Methyl Orange with Nanoscale Zerovalent Iron Particles, Journal of Environmental Engineering and Management, 2010; 20: 137-143.
19. Yang-hsin, Shih Meng-Yi, Chen Yuh-Fan, Su (2011) Pentachlorophenol reduction by Pd/Fe bimetallic nanoparticles: Effects of copper nickel and ferric cations. Applied Catalysis B: Environmental 105(1-2) 24-29 10.1016/j.apcatb.2011.03.024
20. Matsumura Y, Hosokawa C, Sasaki-Mori M, Akahira A, Fukunaga K, Ikeuchi T, et al. Isolation and characterization of novel bisphenol-A-degrading bacteria from soils. Biocontrol Sci. 2009;14:161–9.
21. Mella B, Benvenuti J, Oliveira RF, Gutterres M. Preparation and characterization of activated carbon produced from tannery solid waste applied for tannery wastewater treatment. Environ Sci Pollut R. 2019;26:6811–7.
22. Hernandez-Abreu AB, Alvarez-Torrellas S, Agueda VI, Larriba M, Delgado JA, Calvo PA, et al. Enhanced removal of the endocrine disruptor compound Bisphenol A by adsorption onto green-carbon materials. Effect of real effluents on the adsorption process. J Environ Manage. 2020;266:110604.
23. Shih YH, Chou SM, Lin CF, Sorption mechanisms of selected chlorinated volatile organic compounds in organoclays, Journal of Environmental Engineering and Management, 2010; 20: 161-168.
24. Mercante LA, Iwaki LEO, Scagion VP, Oliveira ON, Mattoso LHC, Correa DS. Electrochemical detection of bisphenol A by tyrosinase immobilized on electrospun nanofibers decorated with gold nanoparticles. Electrochem. 2021;2:41–9.
25. Park CM, Heo J, Yoon Y. Oxidative degradation of bisphenol A and 17 α-ethinyl estradiol by Fenton-like activity of silver nanoparticles in aqueous solution. Chemosphere. 2017;168:617–22.
26. Krajangpan S, Jarabek L, Jepperson J, Chisholm B, Bezbaruah A. Polymer modified iron nanoparticles for environmental remediation. Polym Prepr. 2008;49:921.
27. Ong CB, Ng LY, Mohammad AW. A review of ZnO nanoparticles as solar photocatalysts: synthesis, mechanisms and applications. Renew Sust Energ Rev. 2018;81:536–51.
28. Majumder S, Chatterjee S, Basnet P, Mukherjee J. ZnO based nanomaterials for photocatalytic degradation of aqueous pharmaceutical waste solutions – a contemporary review. Environ Nanotechnol Monit Manage. 2020;14:100386.
29. Wei-Szu, Liu Yu-Huei, Peng Chia-En, Shiung Yang-hsin, Shih (2012) The effect of cations on the aggregation of commercial ZnO nanoparticle suspension. Journal of Nanoparticle Research 14(12) 10.1007/s11051-012-1259-9
30. Yu-Huei, Peng Chih-ping, Tso Yi-chun, Tsai Cheng-ming, Zhuang Yang-hsin, Shih (2015) The effect of electrolytes on the aggregation kinetics of three different ZnO nanoparticles in water. Science of The Total Environment 530-531183-190 10.1016/j.scitotenv.2015.05.059
31. Yu-Huei, Peng Yi-Chun, Tsai Chia-En, Hsiung Yi-Hsuan, Lin Yang-hsin, Shih (2017) Influence of water chemistry on the environmental behaviors of

commercial ZnO nanoparticles in various water and wastewater samples. Journal of Hazardous Materials 322348-356 10.1016/j.jhazmat.2016.10.003
32. Wang YJ, Hu K, Yang ZY, Ye CL, Li X, Yan K. Facile synthesis of porous ZnO nanoparticles efficient for photocatalytic degradation of biomass-derived bisphenol A under simulated sunlight irradiation. Front Bioeng Biotech. 2021;8:616780.
33. Kazeminezhad I, Sadollahkhani A. Influence of pH on the photocatalytic activity of ZnO nanoparticles. J Mater Sci-Mater El. 2016;27:4206–15.
34. Lee KM, Lai CW, Ngai KS, Juan JC. Recent developments of zinc oxide based photocatalyst in water treatment technology: a review. Water Res. 2016;88: 428–48.
35. Zhao X, Du PH, Cai ZQ, Wang T, Fu J, Liu W. Photocatalysis of bisphenol A by an easy-settling titania/titanate composite: effects of water chemistry factors, degradation pathway and theoretical calculation. Environ Pollut. 2018;232:580–90.
36. Zerjav G, Albreht A, Vovk I, Pintar A. Revisiting terephthalic acid and coumarin as probes for photoluminescent determination of hydroxyl radical formation rate in heterogeneous photocatalysis. Appl Catal A-Gen. 2020;598: 117566.
37. Deokar PS, Cremaschi L. Effect of nanoparticle additives on the refrigerant and lubricant mixtures heat transfer coefficient during in-tube single-phase heating and two-phase flow boiling. Int J Refrig. 2020;110:142–52.
38. Choi K, Kang T, Oh SG. Preparation of disk shaped ZnO particles using surfactant and their PL properties. Mater Lett. 2012;75:240–3.
39. Sahu RS, Shih YH. Reductive debromination of tetrabromobisphenol A by tailored carbon nitride Fe/Cu nanocomposites under an oxic condition. Chem Eng J. 2019;378:122059.
40. Sahu RS, Bindumadhavan K, Doong RA. Boron-doped reduced graphene oxide-based bimetallic Ni/Fe nanohybrids for the rapid dechlorination of trichloroethylene. Environ Sci-Nano. 2017;4:565–76.
41. Trandafilovic LV, Jovanovic DJ, Zhang X, Ptasinska S, Dramicanin MD. Enhanced photocatalytic degradation of methylene blue and methyl orange by ZnO:Eu nanoparticles. Appl Catal B-Environ. 2017;203:740–52.
42. Zeng Y, Guo N, Xu XJ, Yu Y, Wang QY, Wang N, et al. Degradation of bisphenol a using peroxymonosulfate activated by WO_3@ MoS_2/Ag hollow nanotubes photocatalyst. Chemosphere. 2019;227:589–97.
43. Chen QF, Wang H, Luan QR, Duan R, Cao XZ, Fang YF, et al. Synergetic effects of defects and acid sites of 2D-ZnO photocatalysts on the photocatalytic performance. J Hazard Mater. 2020;385:121527.
44. Saffari R, Shariatinia Z, Jourshabani M. Synthesis and photocatalytic degradation activities of phosphorus containing ZnO microparticles under visible light irradiation for water treatment applications. Environ Pollut. 2020; 259:113902.
45. Sahu RS, Shih YH, Chen WL. New insights of metal free 2D graphitic carbon nitride for photocatalytic degradation of bisphenol A. J Hazard Mater. 2021; 402:123509.
46. French RA, Jacobson AR, Kim B, Isley SL, Penn RL, Baveye PC. Influence of ionic strength, pH, and cation valence on aggregation kinetics of titanium dioxide nanoparticles. Environ Sci Technol. 2009;43:1354–9.
47. Fatisson J, Domingos RF, Wilkinson KJ, Tufenkji N. Deposition of TiO_2 Nanoparticles onto silica measured using a quartz crystal microbalance with dissipation monitoring. Langmuir. 2009;25:6062–9.
48. Liu W, Yang Q, Wang Z, Lv XF, Yang ZL. Photocatalytic degradation of trichloroethylene over BiOCl under UV irradiation. Appl Organomet Chem. 2018;32:e4354.
49. Wang P, Yang SY, Shan L, Niu R, Sha XT. Involvements of chloride ion in decolorization of Acid Orange 7 by activated peroxydisulfate or peroxymonosulfate oxidation. J Environ Sci-China. 2011;23:1799–807.
50. Qu JG, Chen RY, Dong X, He JX. Effect of NaCl concentrations on the photodecoloration of reactive azo-dyes and their cotton dyeings. Text Res J. 2014;84:2140–8.
51. Toledo IB, Ferro-Garcia MA, Rivera-Utrilla J, Moreno-Castilla C, Fernandez FJV. Bisphenol A removal from water by activated carbon. Effects of carbon characteristics and solution chemistry. Environ Sci Technol. 2005;39:6246–50.
52. Garcia-Espinoza JD, Zolfaghari M, Nacheva PM. Synergistic effect between ultraviolet irradiation and electrochemical oxidation for removal of humic acids and pharmaceuticals. Water Environ J. 2020;34:232–46.

Publisher's Note